

Transferable Belief Model on Quantum Circuits

Qianli Zhou, Hao Luo, Lipeng Pan, Yong Deng*, Éloi Bossé, *Senior Member, IEEE*

Abstract—The transferable belief model, a semantic interpretation of Dempster-Shafer theory, enables agents to reason and make decisions in environments that are imprecise and incomplete. The model provides distinct semantics for managing unreliable testimonies, facilitating a more rational and general process of belief transfer than the Bayesian approach. However, because both the belief masses and the structure of the focal sets must be taken into account when updating belief functions—introducing additional computational complexity during reasoning—the transferable belief model has gradually fallen out of favor in recent research. In this paper, we implement the transferable belief model on quantum circuits, demonstrating that belief functions provide a more concise and effective alternative to Bayesian approaches within the quantum computing framework. Furthermore, by leveraging the unique characteristics of quantum computing, we propose several novel approaches for belief transfer. More broadly, this paper introduces a novel perspective on basic information representation in quantum AI models, proposing that belief functions are better suited than Bayesian approaches for handling uncertainty in quantum circuits.

Index Terms—quantum computing, Dempster-Shafer theory, information fusion, transferable belief model, quantum AI

I. INTRODUCTION

IMPLEMENTING **trustworthy**, **interpretable** and **generalizable** reasoning approaches in uncertain environment is the key issue for the contemporary AI developments. Dempster-Shafer (DS) theory of evidence, also known as belief function theory, is an effective tool for modeling restrictions of variable in uncertain environments [1]. Initially introduced through multi-valued mappings in probability spaces, it has since been interpreted and extended to various semantic frameworks. The transferable belief model (TBM) [2] is the most well-known of these, independent of probability theory, and provides a complete, rigorous, and elegant theoretical system for subjective belief representation. In the realm of the **trustworthy**, the TBM offers a distinct interface for unreliable testimonies, allowing a single information granule to represent both the randomness of the variables and the ambiguity of the knowledge state. In the realm of the **interpretable**, the TBM consists of two levels: the credal level and the pignistic level. The credal level facilitates the transfer of the agent’s

This work is partially supported by the National Natural Science Foundation of China (Grant No. 62373078).

Qianli Zhou was with School of Electronics and Information, Northwestern Polytechnical University, Xi'an 710072, China.

Hao Luo and Yong Deng were with the Institute of Fundamental and Frontier Science, University of Electronic Science and Technology of China, Chengdu 610054, China.

Lipeng Pan was with the College of Information Engineering, Northwest A&F University, Yangling, 712100, China.

Éloi Bossé was with the Department of Image and Information Processing, IMT-Atlantique, Brest, 29238, France, also with the Expertises Parafuse, Quebec City, G1W 4N1, Canada.

belief state using available information, while the pignistic level makes decisions based on the current belief state. In the realm of the **generalizable**, the TBM serves as a bridge between probabilistic and possibilistic information, enabling belief functions to model both statistical data and linguistic knowledge. Therefore, the belief function theory, developed from the TBM semantics is widely used in multi-source information fusion [3]–[5], expert decision making [6], [7], fault diagnosis [8], [9], classifier fusion [10] and computer vision [11], [12]. However, these approaches typically represent data and knowledge as belief functions using general machine learning methods that perform evidential operations on high-level information representations or small-scale data sets. This is because belief functions, as information granules modeled on the power set [13], introduce extra computational complexity. In other words, the advantages of using belief functions are outweighed by the burden of increased computational complexity. Thus, in the recent wave of Artificial Generative Intelligence development, the advantages of belief functions have been overshadowed by scaling law driven by the high computational power.

Quantum computing, an emerging research frontier in recent years, seeks to harness the principles of quantum mechanics to enable an operation distinct from classical information processing [14]. Its outstanding performance on specific complex problems has inspired its adoption in the field of machine learning [15]–[17], with the aim of addressing current challenges such as dimensionality explosion and optimization difficulties. However, in recent years, as more machine learning algorithms have been quantized [18]–[20], scholars have found that quantum machine learning offers no significant advantage in algorithmic acceleration [21]. In the context of NISQ, the development of generalizable quantum AI methods appears to have encountered yet another bottleneck [22], [23]. In quantum computing, information is stored in the wave function and can only be extracted through measurements. Unlike Kolmogorov’s probability axioms, quantum probability is based on von Neumann’s measurement theory, where the probability of a quantum state is determined by the square of its amplitude [24]. Thus, when classical probabilistic information is transferred directly to quantum computing for processing, a significant difference emerges in how information is updated: **From updating the probabilities of basic events in classical systems to updating the probabilities of quantum states through the manipulation of qubits.** However, in previous research on quantum machine learning, scholars seem to have overlooked these implications. The basic probability assignment (BPA)¹, an identical information

¹Also referred to as basic belief assignment in TBM.

content representation of belief function, can be viewed as a 2^n -dimensional normalized weight vector. When a BPA is encoded in a quantum superposition state, each element can be associated with a qubit, this consistency does not exist in probabilistic semantics [25].

The intersection of quantum mechanics and Dempster-Shafer theory has been explored by various scholars from different perspectives, such as lattice of subspace [26], quantum-like [27], quantum modeling [28], [29], mixed-pure state [30], and interference prediction [31]. However, these methods do not take advantage of the consistency relationship between qubits and elements under the belief function framework. Zhou *et al.* encoded the BPA into a quantum state using element-qubit consistency and extended conventional belief operations via the HHL algorithm [25] and the variational quantum linear solver [32]. This demonstrates that belief function operations on quantum circuits can inherit the general advantages of quantum machine learning. More generally, evidence combination rules based on Boolean algebra have been extended to quantum circuits, and attribute fusion-based evidential classifiers have been implemented, demonstrating exponential complexity advantages over classical approaches [33]. Thus, an open issue arises: **Does the belief function-based approaches on quantum circuits have unique advantages over general quantum AI methods?** In this paper, we will try to address this issue by developing the TBM on quantum circuits. First, we will implement the TBM on quantum circuits and modify specific operations to better adapt them to quantum computing. Next, we will harness the unique characteristics of quantum computing to enhance the TBM, particularly by exploring belief operations that have been overlooked in classical contexts. Finally, we will discuss why belief functions provide distinct advantages in quantum computing.

The structure of the paper is organized as follows: Section II introduces the necessary concepts in TBM and quantum computing. Section III represents and implements the belief function on quantum circuits. Section IV discusses the operations of credal level on quantum circuits and proposes some belief revision methods inspired by the quantum computing. Section V extends the operations on product space on quantum space. Section VI summarizes the contributions and discusses potential directions for future research.

II. PRELIMINARIES

A. Transferable belief model

The transferable belief model (TBM) is an interpretation of Dempster-Shafer theory that quantifies an agent's belief at a certain time. During the development of TBM [2], although the authors acknowledged that its semantics are similar to Shafer's original work on evidence theory [34], they emphasized a clear distinction between belief functions and probabilities to avoid confusion. In later developments, since the two models (TBM and evidence theory) share many operations with similar semantics, no specific distinction is typically made between them in cases where their relationship to probability theory is not emphasized. In this paper, we will use widely accepted

notations, even if they differ from those originally proposed in the TBM.

1) *Information representation:* Consider an uncertain variable X , whose true value is contained within the frame of discernment (FOD) $\Omega = \{\omega_1, \dots, \omega_n\}$. The belief (Bel) function $Bel : 2^\Omega \rightarrow [0, 1]$, which satisfies $\forall F_1, F_2, \dots, F_k \subseteq \Omega, Bel(F_1 \cup F_2 \cup \dots \cup F_k) \geq \sum_i Bel(F_i) - \sum_{i>j} Bel(F_i \cap F_j) + \dots + (-1)^n Bel(F_1 \cap F_2 \cap \dots \cap F_k)$, represents a restriction of X , i.e., it conveys information about the value of X . $Bel(F_i)$ represents the agent's support belief that $X \in F_i$. Its dual measure, plausibility function, is denoted as $Pl(F_i) = 1 - Bel(\bar{F}_i)$, which represents the agent's non-negative belief that $X \in F_i$. Bel and Pl functions represents the lower and upper beliefs of the proposition. A mass function m , called basic probability assignment (BPA), is an identical information representation of them, which satisfies $m(F_i) \in [0, 1]$ and $\sum_{F_i \subseteq \Omega} m(F_i) = 1$. If $m(F_i) > 0$, F_i is a focal set, and i is the decimal representation of binary codes of F_i . They have the following reversible transformations: [34]–[36]

$$\begin{aligned} Bel(F_i) &= \sum_{\emptyset \neq F_j \subseteq F_i} m(F_j), Bel(\emptyset) = 0; \\ m(F_i) &= \sum_{F_j \subseteq F_i} (-1)^{|F_i|-|F_j|} Bel(F_j), m(\emptyset) = 1 - Bel(\Omega). \\ Pl(F_i) &= \sum_{F_i \cap F_j \neq \emptyset} m(F_j), Pl(\emptyset) = 0; \\ m(F_i) &= \sum_{F_j \subseteq F_i} (-1)^{|F_i|-|F_j|+1} Pl(\bar{F}_j), m(\emptyset) = 1 - Pl(\Omega). \end{aligned}$$

In addition, derived via the set operations, there are another two dual identical information representations, implicability b function and commonality q function, which are defined as

$$\begin{aligned} b(F_i) &= \sum_{F_j \subseteq F_i} m(F_j); m(F_i) = \sum_{F_j \subseteq F_i} (-1)^{|F_i|-|F_j|} b(F_j). \\ q(F_i) &= \sum_{F_i \subseteq F_j} m(F_j); m(F_i) = \sum_{F_i \subseteq F_j} (-1)^{|F_j|-|F_i|} q(F_j). \end{aligned}$$

For the programming convenience, the BPA can be represented as the vector form $\mathbf{m} = [m(F_0), \dots, m(F_{2^n-1})]^T$, and the above functions can be implemented through the matrix calculus [35]:

$$\begin{aligned} \mathbf{b} &= \mathbf{m} \mathbf{2} \mathbf{b} \cdot \mathbf{m}, m2b(F_i, F_j) = \begin{cases} 1 & F_j \subseteq F_i \\ 0 & \text{others} \end{cases}; \\ \mathbf{q} &= \mathbf{m} \mathbf{2} \mathbf{q} \cdot \mathbf{m}, m2q(F_i, F_j) = \begin{cases} 1 & F_i \subseteq F_j \\ 0 & \text{others} \end{cases}. \end{aligned} \quad (1)$$

2) *Credal level:* When the agent possesses multiple bodies of evidence from different sources, at the credal level, the agent's belief is transferred to integrate the available information. When the sources are independent and reliable, the conjunctive combination rule (CCR), also known as the unnormalized Dempster's rule of combination, provides a reasonable manner to integrate them. CCR can be implemented through BPA or q function [36]:

$$m_{1\odot_2}(F_i) = \sum_{F_j \cap F_k = F_i} m_1(F_j)m_2(F_k), \quad q_{1\odot_2}(F_i) = q_1(F_i)q_2(F_i). \quad (2)$$

According to the Eq. (1), the CCR also can be implemented through matrix calculus: $\mathbf{m}_{1\odot_2} = \mathbf{S}_{\mathbf{m}_2} \cdot \mathbf{m}_1$, where $\mathbf{S}_{\mathbf{m}_2} = \mathbf{m}_2 \mathbf{q}^{-1} \mathbf{diag}(\mathbf{q}_2) \mathbf{m}_2 \mathbf{q}$. When the sources are independent and at least one of them is reliable, the disjunctive combination rule (DCR) provides a reasonable choice, whose implementations are [35]:

$$m_{1\odot_2}(F_i) = \sum_{F_j \cup F_k = F_i} m_1(F_j)m_2(F_k), \quad b_{1\odot_2}(F_i) = b_1(F_i)b_2(F_i). \quad (3)$$

Building on the above, and driven by specific requirements in information fusion, a parametric matrix calculus-based combination rule, called the α -junction, is proposed [35], [37], which is denoted as

$$\mathbf{m}_{1\odot_2^\alpha} = \mathbf{K}_{\mathbf{m}_2}^{\cap, \alpha} \cdot \mathbf{m}_1, \quad \mathbf{m}_{1\odot_2^\alpha} = \mathbf{K}_{\mathbf{m}_2}^{\cup, \alpha} \cdot \mathbf{m}_1. \quad (4)$$

The conjunctive case \odot^α means the neutral element is m_Ω , i.e., $m \odot^\alpha m_\Omega = m$, and the $\mathbf{K}_m^{\cap, \alpha}$ is denoted as

$$\mathbf{K}_m^{\cap, \alpha} = \sum_{F_i \subseteq \Omega} m(F_i) \cdot \mathbf{K}_{F_i}^{\cap, \alpha}, \quad \mathbf{K}_{F_i}^{\cap, \alpha} = \begin{cases} \mathbf{I} & F_i = \Omega, \\ \prod_{\omega \notin F_i} \mathbf{K}_{\omega}^{\cap, \alpha} & F_i \subset \Omega, \end{cases}$$

$$\mathbf{K}_\omega^{\cap, \alpha}(F_i, F_j) = \begin{cases} 1 & \omega \notin F_i, F_j = F_i \cup \{\omega\}, \\ \alpha & \omega \notin F_j, F_i = F_j, \\ 1 - \alpha & \omega \notin F_j, F_i = F_j \cup \{\omega\}, \\ 0 & \text{others,} \end{cases}$$

where $\alpha \in [0, 1]$, the boundary cases are as follows: when $\alpha = 1$ degrades to the CCR, and $\alpha = 0$ degrades to the conjunctive exclusive combination rule (CECR):

$$m_1 \odot m_2(F_i) = \sum_{F_i = (F_j \cap F_k) \cup (\overline{F_j} \cap \overline{F_k})} m_1(F_j)m_2(F_k). \quad (6)$$

Similarly, the disjunctive case \odot^α means the neutral element is m_\emptyset , i.e., $m \odot^\alpha m_\emptyset = m$, and the $\mathbf{K}_m^{\cup, \alpha}$ is denoted as

$$\mathbf{K}_m^{\cup, \alpha} = \sum_{F_i \subseteq \Omega} m(F_i) \cdot \mathbf{K}_{F_i}^{\cup, \alpha}, \quad \mathbf{K}_{F_i}^{\cup, \alpha} = \begin{cases} \mathbf{I} & F_i = \emptyset, \\ \prod_{\omega \in F_i} \mathbf{K}_{\omega}^{\cup, \alpha} & F_i \in 2^\Omega \setminus \emptyset, \end{cases}$$

$$\mathbf{K}_\omega^{\cup, \alpha}(F_i, F_j) = \begin{cases} 1 & \omega \notin F_j, F_i = F_j \cup \{\omega\}, \\ \alpha & \omega \in F_j, F_i = F_j, \\ 1 - \alpha & \omega \notin F_i, F_j = F_i \cup \{\omega\}, \\ 0 & \text{others,} \end{cases}$$

where $\alpha \in [0, 1]$, the boundary cases are as follows: when $\alpha = 1$ degrades to the DCR, and $\alpha = 0$ degrades to the disjunctive exclusive combination rule (DECR):

$$m_1 \odot m_2(F_i) = \sum_{F_i = (F_j \cap \overline{F_k}) \cup (\overline{F_j} \cap F_k)} m_1(F_j)m_2(F_k). \quad (8)$$

As the outcomes are derived from the required properties, the interpretation of the α -junction remains an open question.

Pichon and Denœux [37] offered an explanation based on the trustworthiness of sources, though it has yet to be applied in specific scenarios.

3) *Pignistic level*: When no additional bodies of evidence are available to update the mass function, belief masses should be assigned to singletons to support decision making, a process known as probability transformation. Driven by the linearity principle, the pignistic probability transformation is defined as [38]

$$BetP_m(\omega) = \sum_{\omega \in F_i} \frac{m(F_i)}{(1 - m(\emptyset))|F_i|}. \quad (9)$$

In addition, several probability transformation methods have been proposed from various perspectives [39]. Among them, the plausibility transformation method, guided by Dempster's semantic consistency, is defined as [40]

$$Pl_P_m(\omega_i) = \frac{pl_m(\omega_i)}{\sum_{\omega_j \in \Omega} pl_m(\omega_j)}, \quad (10)$$

where $pl_m(\omega) = Pl(\{\omega\})$, and it is denoted as the contour function.

4) *Operations on product space*: Operating belief function on product space [41] is the key issue for both the Generalized Bayesian Theorem (GBT) [42] and the Valuation-Based System (VBS) [43]. Consider a mass function m on the space $\Omega \times \Theta$, denoted as $m^{\Omega \times \Theta}$, its marginalization on the FoD Ω is

$$m^{\Omega \times \Theta \downarrow \Omega}(F_i) = \sum_{\{G_i \subseteq \Omega \times \Theta \mid \text{Proj}(G_i \downarrow \Omega) = F_i\}} m^{\Omega \times \Theta}(G_i), \quad (11)$$

$$\text{Proj}(G_i \downarrow \Omega) = \{F_i \subseteq \Omega \mid \exists H_i \subseteq \Theta, F_i \times H_i = G_i\}.$$

The inverse operation of marginalization, representing the mass function m^Ω on the FoD $\Omega \times \Theta$, is known as the vacuous extension, which is defined as

$$m^{\Omega \uparrow \Omega \times \Theta}(G_i) = \begin{cases} m^\Omega(F_i) & F_i \subseteq \Omega, G_i = F_i \times \Theta, \\ 0 & \text{others.} \end{cases} \quad (12)$$

Hence, for the mass functions from different FoDs, such as m_1^Ω and m_2^Θ , their combination and projection can be implemented as $m_1^{\Omega \odot_2} = (m_1^{\Omega \times \Theta} \odot m_2^{\Omega \times \Theta}) \downarrow \Omega$, $m_1^{\Theta \odot_2} = (m_1^{\Omega \times \Theta} \odot m_2^{\Omega \times \Theta}) \downarrow \Theta$. When one of the mass functions is categorical, meaning it has only one focal set, the CCR in this case is referred to as the conditioning of the mass function. When given the target element of Θ locating in H_i , the conditioning of m^Ω is $m^\Omega[H_i] = (m^{\Omega \times \Theta} \odot m_{H_i}^{\Omega \times \Theta}) \downarrow \Omega$, $m_{H_i} \equiv \{m(H_i) = 1\}$. The inverse operation of conditioning is known as the ballooning extension, which entails providing $m^\Omega[H_i]$ and extending it onto the FoD $\Omega \times \Theta$. It is defined as

$$m^\Omega[H_i] \uparrow \Omega \times \Theta(G_i) = \begin{cases} m^\Omega[H_i](F_i) & G_i = (F_i \times H_i) \cup (\Omega \times (\Theta \setminus H_i)), F_i \subseteq \Omega, \\ 0 & \text{others.} \end{cases} \quad (13)$$

The core contribution of this paper is the implementation of these methods on quantum circuits to quantize the TBM.

B. Quantum computing

Quantum computing is governed by the four fundamental principles of quantum mechanics and seeks to perform information updates through the evolution of quantum states [44]. To assist readers unfamiliar with quantum computing in understanding the contributions of this paper, we will introduce key concepts of quantum computing based on these four principles.

1) *Quantum state*: Any isolated quantum system can be fully described by a state vector $|\psi\rangle$ in a complex Hilbert space, which encapsulates all the information about the system. This state vector is expressed as a superposition of basis states, and the computational basis states of qubits are $|0\rangle$ and $|1\rangle$. Consider an information system represented by n bits. In classical computing, information is modeled as an n -dimensional binary string, whereas in quantum computing, the state of information is represented as a vector composed of all possible n -dimensional binary strings. It can be written as

$$|\psi\rangle \equiv a_0 |0\rangle^n + a_1 |0\rangle^{n-1} |1\rangle + \cdots + a_{2^n-1} |1\rangle^n = \begin{bmatrix} a_0 \\ \vdots \\ a_{2^n-1} \end{bmatrix},$$

and it has $\|a_0\|^2 + \|a_1\|^2 + \cdots + \|a_{2^n-1}\|^2 = 1$. For existing multiple quantum states, they can be composed using the tensor product, which is written as $|\psi_0\rangle \otimes |\psi_1\rangle \otimes \cdots \otimes |\psi_k\rangle = |\psi_0\psi_1\cdots\psi_k\rangle$.

2) *Quantum evolution*: The time evolution of a closed quantum system is governed by a unitary operator U . If a quantum state $|\psi\rangle$ evolves to a state $|\psi'\rangle$ at time $t \rightarrow t'$, then $|\psi'\rangle = U_{t \rightarrow t'} |\psi\rangle$. $U_{t \rightarrow t'}$ is an unitary matrix, which leads the evolution being deterministic and reversible. Quantum gates, also known as the operators, act on quantum states to represent the quantum evolution. Table I shows the necessary quantum gates in this paper.

TABLE I
NECESSARY QUANTUM GATES IN THIS PAPER, WHERE I_n IS AN n -DIMENSIONAL ELEMENTARY MATRIX.

X gate	RY gate	C-NOT gate	Toffoli gate	Control-RY gate
$[X]$	$[R_Y(\theta)]$	$c \cdot \begin{smallmatrix} \oplus \\ t \end{smallmatrix}$	$c \cdot \begin{smallmatrix} \oplus \\ t \end{smallmatrix}$	$c \cdot \begin{smallmatrix} \oplus \\ t \end{smallmatrix} [R_Y(\theta)]$
$\begin{bmatrix} 0 & 1 \\ 1 & 0 \end{bmatrix}$	$\begin{bmatrix} \cos \frac{\theta}{2} & \sin \frac{\theta}{2} \\ -\sin \frac{\theta}{2} & \cos \frac{\theta}{2} \end{bmatrix}$	$[I_2 \ 0]$	$[I_6 \ 0]$	$[I_2 \ 0]$

3) *Quantum measurement*: In a quantum system, physical quantities are measured through their associated operators (Hermitian matrices). The result of the measurement will be one of the operator's eigenvalues, and after the measurement, the system will collapse into the corresponding eigenstate (the eigenvector associated with the measured eigenvalue). In quantum computing, measurements are typically performed in the computational basis. The measurement operators are used to extract the probability information of the quantum state in the $|0\rangle$ and $|1\rangle$ states (for single-qubit systems) or the standard basis states (such as $|00\rangle$, $|01\rangle$, etc., for multi-qubit systems). After the measurement, the quantum state collapses to the corresponding computational basis state. For a quantum superposition state, the probability of obtaining a particular outcome is given by the square of the amplitude of that state.

For example, for the state $|\psi\rangle = a|0\rangle + b|1\rangle$, the outcome of measurement is $Prob(|1\rangle) = \|b\|^2$.

4) *Quantum entanglement*: Quantum entanglement is one of the key advantages of quantum computing, enabling connections between qubits that surpass classical limitations. In a multi-qubit system with entanglement, measuring the amplitude of each qubit individually and then composing them via tensor products yields a different outcome compared to measuring all qubits together. For example, the Bell state $|\Phi^+\rangle = a|00\rangle + b|11\rangle$ is an entangled state. In quantum computing, gates involving control and target qubits are responsible for generating entanglement during quantum evolution.

Secs. II-B1–II-B4 review the essentials: an n -qubit state encodes 2^n basis states, unitary operators update amplitudes/phases, projective measurements extract probabilities irreversibly, and controlled operations generate entanglement—together defining the quantum computing paradigm.

III. REPRESENTING AND IMPLEMENTING BELIEF FUNCTION ON QUANTUM CIRCUITS

A. Motivation

The encoding method is proposed in [25], and in this paper, we reorganize the logic of motivation with the aim of emphasizing that **this quantization is not simply an extension but a necessary research**. A mass function can be viewed as a random set, that is, a collection of sets with inherent randomness, where the randomness is modeled by a probability distribution. Similarly, a quantum superposition state can be interpreted as an uncertain state, which is revealed through measurement and characterized by the probabilistic uncertainty. Additionally, for an n -element FoD, belief masses are assigned to its power set, and for an n -qubit system, the quantum superposition state is composed of 2^n states. Fig. 1 shows the extension process of classical bit to the superposition state and random sets. Despite their distinct mathematical consistency, this interesting relation has not been discussed in prior research.

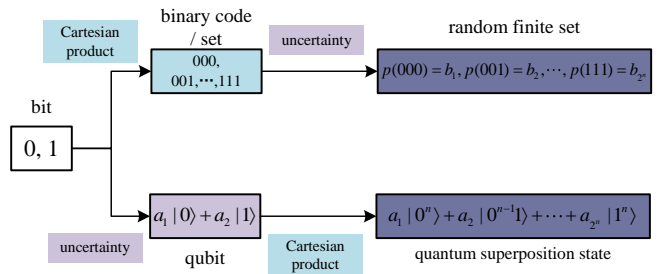


Fig. 1. Motivation of encoding mass function on quantum circuits.

B. Encoding mass function as superposition state

We map the elements in the FoD to qubits, focal sets to states, mass function to superposition state, and belief masses to the probabilities obtained after measurement.

Definition 1: Consider a mass function m with a FoD $\Omega = \{\omega_1, \dots, \omega_n\}$, an n -qubit system q_0, \dots, q_{n-1} can model its uncertainty as a quantum superposition state, called mass function quantum state (MFQS) $|m\rangle$, which is denoted as

$$|m\rangle = \sum_{F_i \subseteq \Omega} \sqrt{m(F_i)} |\text{bin}(i)\rangle, \quad (14)$$

where $\text{bin}(i)$ indicates the binary codes of i . The focal set F_i corresponds to the state $|\text{bin}(i)\rangle$, whether the ω_j contained is represented by the state of the qubit q_{j-1} .

Remark 1: Von Neumann's measurement theory of quantum probability focuses on the likelihood of a state resulting from the measurement of a quantum system, which corresponds to mutually exclusive events in Kolmogorov's probability axioms. However, in the belief function framework, the focal sets may be non-exclusive with each other. They represent ignorance on the target element by allowing mutually exclusive elements to form a proposition (focal set). Thus, encoding focal sets as orthogonal states in Eq. (14) does not fully align with the original physical interpretation. However, this inconsistency does not affect the development of computational advantages on quantum circuits through their mathematical correspondences.

Remark 2: The encoding ensures that the belief masses correspond to the probabilities after measurement, and is therefore only related to the amplitude. Consequently, although quantum states are represented in Hilbert space, the MFQS is not connected to existing research in complex-valued evidence theory [45], [46], which emphasizes the use of phase information to model additional types of uncertainty.

C. Implementation of mass function quantum state

In [25], Zhou *et al.* provide a method for quantizing the general mass functions. Consider a mass function m with a FoD Ω , its MFQS $|m\rangle$ can be implemented in an n -qubit system:

- **Initialization.** Start from the ground state $|\psi_0\rangle = |0\rangle^{\otimes n}$. Apply $X^{\otimes n}$ so that each qubit is flipped to $|1\rangle$:

$$|\psi_1\rangle = X^{\otimes n} |0\rangle^{\otimes n} = |1\rangle^{\otimes n}.$$

- **Uniformly controlled rotations.** For each qubit q_k ($k = 0 : n - 1$), apply the controlled operation

$$U_k = \sum_{t=0}^{2^k-1} (|t\rangle\langle t|)_{0:k-1} \otimes R_Y(\theta_{k,t})_k.$$

After acting on $|\psi_1\rangle$, the system evolves as $|\psi_{k+1}\rangle = U_k |\psi_k\rangle$, where t denotes the computational branch determined by the first k qubits.

- **Angle selection.** For each branch t , define the partial sums

$$S_{k,t}^{(1)} = \sum_{F: \text{prefix}(F,k)=t, \omega_{k+1} \in F} m(F), \quad S_{k,t}^{(0)} = \sum_{F: \text{prefix}(F,k)=t, \omega_{k+1} \notin F} m(F).$$

The rotation angle is chosen by $\tan^2\left(\frac{\theta_{k,t}}{2}\right) = \frac{S_{k,t}^{(0)}}{S_{k,t}^{(1)}}$, ensuring that along branch t , the measurement probability ratio matches

$$\Pr[\omega_{k+1} \notin F] : \Pr[\omega_{k+1} \in F] = S_{k,t}^{(0)} : S_{k,t}^{(1)}.$$

- **Final state.** After all controlled rotations, the system reaches

$$|\psi_{\text{final}}\rangle = \left(\prod_{k=0}^{n-1} U_k \right) X^{\otimes n} |0^n\rangle,$$

where the amplitudes encode the mass function $m(\cdot)$:

$$|\langle F | \psi_{\text{final}} \rangle|^2 = m(F).$$

Fig. 2 shows the implementation circuits for a mass function under a 3-element FoD. While this method can encode an arbitrary mass function as a quantum state, it suffers from high computational complexity and is not suitable for quantizing evidential reasoning methods.

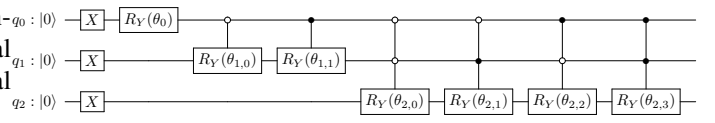


Fig. 2. Implementation of MFQS with a 3-qubit system.

In this paper, we present an efficient method for preparing a specific type of mass function, known as the poss-transferable mass function, which corresponds classically to an invertible transformation from the possibility distribution to the belief function [47].

Definition 2: Consider a possibility distribution π under an n -element FoD, the poss-transferable mass function is defined as

$$m_{\text{Poss}}(F_i) = \prod_{\omega \in F_i} \pi(\omega) \prod_{\omega \notin F_i} (1 - \pi(\omega)) = \bigcap_{\omega \in \Omega} \{\Omega \setminus \{\omega\}\}^{\pi(\omega)}, \quad (15)$$

where $F_i^\sigma \equiv \{m(F_i) = 1 - \sigma, m(\Omega) = \sigma\}$ is called the simple mass function. This transformation is developed from the inverse process of canonical decomposition. Hence, when the outcome of the canonical decomposition of m is a possibility distribution, m will be a poss-transferable mass function.

Theorem 1: For an n -element FoD, the quantum state of a poss-transferable mass function can be implemented using exactly n single-qubit R_Y gates, with rotation parameters determined by its contour function.

Proof 1: Please refer to the supplementary material.

Remark 3: Quantum states of the poss-transferable mass function are equivalent to separable quantum states in quantum initial state preparation, i.e., quantum states without entanglement.

Remark 4: Although both the poss-transferable mass function and the consonant mass function can be uniquely transformed into a possibility distribution, they originate from different perspectives. The specific differences in their properties are analyzed in detail in [47].

D. Implementation of belief functions on quantum circuits

As shown in Section II-A1, there are some identical information content representations with mass functions, which can model uncertainty more intuitively and combine bodies of evidence more conveniently. Matrix calculus is an effective approach for implementing them in programming. In quantum computing, they can be efficiently extracted from MFQS using control gates ².

Definition 3: Let $|m\rangle$ be a MFQS encoded in an n -qubit system with data qubits q_0, \dots, q_{n-1} , and let q_n be an ancilla qubit initialized in $|0\rangle$. We denote by $C^{\mathcal{C}(F)}X(q_n)$ ³ the multi-controlled X gate acting on q_n , triggered when all conditions in $\mathcal{C}(F)$ are satisfied. Then, the evolution of the state is:

$$\begin{aligned} |\psi_0\rangle &= |m\rangle |0\rangle, \\ |\psi_1\rangle &= C^{\mathcal{C}(F_i)}X(q_n)|\psi_0\rangle \rightarrow \\ &= |m\rangle \left(\sqrt{\sum_{F_i \subseteq F_j} m(F_j)} |1\rangle + \sqrt{\sum_{F_i \cap \bar{F}_j \neq \emptyset} m(F_j)} |0\rangle \right) \\ &= |m\rangle \left(\sqrt{q(F_i)} |1\rangle + \sqrt{\sum_{F_i \cap \bar{F}_j \neq \emptyset} m(F_j)} |0\rangle \right), \\ |\psi_2\rangle &= C^{\mathcal{C}(\bar{F}_i)}X(q_n)|\psi_0\rangle \rightarrow \\ &= |m\rangle \left(\sqrt{\sum_{F_j \subseteq F_i} m(F_j)} |1\rangle + \sqrt{\sum_{F_j \cap F_i \neq \emptyset} m(F_j)} |0\rangle \right) \\ &= |m\rangle \left(\sqrt{b(F_i)} |1\rangle + \sqrt{Pl(\bar{F}_i) - m(\emptyset)} |0\rangle \right). \end{aligned}$$

The specific quantum circuits are shown in Fig. 3.

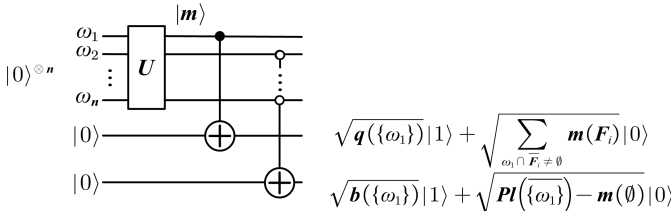


Fig. 3. Implementation of belief functions on quantum circuits.

Therefore, the transformation method defined based on the inclusion relation of focal sets can be efficiently implemented on quantum circuits. Operations in quantum computing are performed on qubits, rather than on states, corresponding in the belief function framework to the focal sets that contain (or do not contain) the corresponding elements. This corresponding relationship is the reason why we should develop TBM on quantum circuits.

²Corresponding expression is incorrect in [48] and has been corrected here.

³For a subset $F_i \subseteq \Omega$, define the *control condition set*

$$\mathcal{C}(F_i) = \{(q_t, 1) \mid \omega_{t+1} \in F_i\}, \mathcal{C}(\bar{F}_i) = \{(q_t, 0) \mid \omega_{t+1} \in \bar{F}_i\},$$

where $(q_t, 1)$ indicates a positive control (activated when $q_t = |1\rangle$), and $(q_t, 0)$ indicates a negative control (activated when $q_t = |0\rangle$).

E. Pignistic level on quantum circuits

In the TBM, the pignistic probability transformation (Eq. (9)) is the most widely recognized method for assigning the belief of multi-element focal sets to their corresponding singletons [38]. Smets has provided an efficient implementation of pignistic transformation through matrices calculus [35], which has been extended on quantum circuits through HHL-inspired method [25]. However, this method does not achieve acceleration and exists the theoretical errors. A quantized approach for pignistic transformation that matches the elegance and efficiency of the credal level remains undiscovered. Therefore, in this paper, we recommend using the plausibility transformation method (Eq. (10)) as the pignistic level of TBM on quantum circuits.

Definition 4: Let $|m\rangle$ be a MFQS encoded on n data qubits q_0, \dots, q_{n-1} , which has been updated at the credal level. Its plausibility transformation on quantum circuits can be realized as follows.

- Introduce n ancilla qubits q_{0a}, \dots, q_{n-1a} initialized in $|0\rangle^{\otimes n}$, so that the joint initial state is $|\psi_0\rangle = |m\rangle |0\rangle^{\otimes n}$.
- For each element $\omega_i \in \Omega$, apply the controlled operation $C^{\mathcal{C}(\{\omega_i\})}X(q_{ia})$. After applying all n such gates, the system evolves as $|\psi_0\rangle |\psi_1\rangle = |m\rangle |m_{pl_m}\rangle$.
- Perform projective measurements on the ancilla register $\{q_{ia}\}$, and record the outcomes in classical bits c_0, \dots, c_{n-1} . The measurement statistics define the contour function: $pl(\omega_i) = \Pr[q_{ia} = 1]$.
- normalize the obtained values to ensure a valid contour representation: $pl(\omega_i) \rightarrow \frac{pl(\omega_i)}{\sum_{\omega_j \in \Omega} pl(\omega_j)}$.

Compared to the pignistic probability transformation, the plausibility transformation method can be efficiently implemented by leveraging the extraction of contour functions on quantum circuits.

F. Discussion

This part primarily introduces how to encode and implement mass functions and their associated representations on quantum circuits. Through a one-to-one correspondence between elements in FoD and qubits in system, operating on each qubit is equivalent to operating on a proposition containing the corresponding element, which is not possible with quantum probability-based information processing methods. These contributions have been presented in our previous works [25] and [33]. To maintain the integrity of this paper, we reorganize the motivation along with the specific evolution and derivation processes. In the following sections, we will further explore this feature and implement additional operations of belief functions on quantum circuits.

IV. CREDAL LEVEL ON QUANTUM CIRCUITS

A. Combination rules for independent sources on quantum circuits

As discussed in Section II, the combination rules for independent sources, such as CCR, DCR, CECR, and DECR, involve handling belief masses and focal sets separately. The fused belief mass is obtained through multiplication, while

the fused focal set is defined using Boolean algebra operations. In quantum computing, state composition is achieved via multiplication, and control-bit gates are used to perform Boolean algebra operations. This naturally raises the question: can we propose a unified rule that encompasses all Boolean algebra operations for independent sources and implement it on quantum circuits?

1) *Boolean algebra-based combination rule:*

Definition 5: Consider k mass functions m_1, \dots, m_k from the independent sources, the Boolean algebra-based combination rule (BACR) of them is defined as

$$m_{k+1}(F_{i_{k+1}}) = \sum_{\mathfrak{B}(F_{i_1}, \dots, F_{i_k}) = F_{i_{k+1}}} \prod_{j=1}^k m_j(F_{i_j}), \quad (16)$$

where m_{k+1} is the result of combination, F_{i_j} is the focal set in the j th body of evidence⁴ and $\mathfrak{B}(F_{i_1}, \dots, F_{i_k})$ is the logical operation of Boolean algebra.

Continue to Definition 5, when $\mathfrak{B}(F_{i_1}, \dots, F_{i_k}) = F_{i_1} \cap \dots \cap F_{i_k}$, BACR reduces to CCR; when $\mathfrak{B}(F_{i_1}, \dots, F_{i_k}) = F_{i_1} \cup \dots \cup F_{i_k}$, it reduces to DCR; when $\mathfrak{B}(F_{i_1}, \dots, F_{i_k}) = (F_{i_1} \cap F_{i_2}) \cup \dots \cup (F_{i_{k-1}} \cap F_{i_k})$, it reduces to the $(K-1)$ -out-of- K rule [49]. Hence, BACR serves as a unified combination rule for independent sources. For categorical inputs (i.e., each mass function has only one focal set), BACR reduces to the classical Boolean algebra operation. To clarify the steps of BACR, we introduce two concepts for Boolean circuit operations.

- **t -layer Boolean algebra operation:** A Boolean algebra operation \mathfrak{B} can be divided into t layers, which corresponds to a t -depth Boolean circuit. Assume that multiple Boolean algebra operations can be performed simultaneously, and t indicates the minimum number of operations required to construct \mathfrak{B} . For example, if $\mathfrak{B} = (\{\omega_1\omega_2\} \cap \{\omega_2\omega_3\}) \cup (\{\omega_2\omega_4\} \cap \{\omega_4\omega_5\})$, $\{\omega_1\omega_2\} \cap \{\omega_2\omega_3\}$ and $\{\omega_2\omega_4\} \cap \{\omega_4\omega_5\}$ can be performed simultaneously, which are denoted as the first layer, and $\{\omega_2\} \cup \{\omega_4\}$ is the second layer. Hence, \mathfrak{B} is a 2-layer Boolean algebra operation, and its corresponding BACR also is denoted as 2-layer BACR.

- **Operation component:** When the output has only one result, the operation corresponding to the maximum number of inputs is called an operation component. Continue to the above example, where $\{\omega_1\omega_2\} \cap \{\omega_2\omega_3\}$ and $\{\omega_2\omega_4\} \cap \{\omega_4\omega_5\}$ are two operation components.

2) *BACR on quantum circuits:* In [25] and [32], the CCR and DCR are implemented on quantum circuits through the HHL algorithm and VQLS, respectively, which realize the specialization and generalization of belief functions. These methods do not utilize the correspondence between elements and qubits; they merely represent a simple migration from the perspective of matrix operations. The fidelity of the implementation outcomes is limited due to the theoretical errors inherent in HHL and VQLS. BACR can be viewed as an extension of Boolean algebra operations from classical sets to random

⁴Special reminder: i_j is a decimal number that can indicate a focal set, and i can no longer be interpreted in isolation.

sets. The Boolean algebra operations of classical sets can be implemented through Boolean circuits, and when randomness is introduced, the idea of extending these Boolean circuits to quantum circuits becomes easily appeared. Hence, in this paper, the combination rules in credal levels are implemented from the perspective of Boolean algebra operation.

Definition 6: Let $\{|m_j\rangle\}_{j=1}^k$ be k MFQSSs, each encoded in an n -qubit system $q_{0_j}, \dots, q_{(n-1)_j}$, where q_{ij} corresponds to the basic element ω_{i+1} in $|m_j\rangle$. The goal state $|m_{k+1}\rangle$ is defined on $q_{0_{k+1}}, \dots, q_{(n-1)_{k+1}}$, representing the outcome of the BACR. For a single operation component in \mathfrak{B} , the state evolution is as follows.

(a) **Negation.** For the complement of $|m_j\rangle$, apply $X^{\otimes n}$:

$$\begin{aligned} X^{\otimes n} |m_j\rangle &= X^{\otimes n} \sum_{F_i \subseteq \Omega} \sqrt{m(F_i)} |\text{bin}(i)\rangle \\ &\longrightarrow \sum_{F_i \subseteq \Omega} \sqrt{m(\overline{F_i})} |\text{bin}(i)\rangle = |\overline{m_j}\rangle. \end{aligned}$$

(b) **Intersection (multi-source CCR).** For the conjunctive combination of $|m_1\rangle, \dots, |m_k\rangle$, the i -th output qubit is obtained via a multi-controlled NOT:

$$|\psi_0\rangle = |m_1\rangle \dots |m_k\rangle |0\rangle, |\psi_1\rangle = C^{\{q_{i_1}, \dots, q_{i_k}\}} X(q_{i_{k+1}}) |\psi_0\rangle \rightarrow |m_1\rangle \dots |m_k\rangle \left(\sqrt{\sum_{F: \omega_{i+1} \in \cap_{j=1}^k F_j} |1\rangle} + \sqrt{\sum_{F: \omega_{i+1} \notin \cap_{j=1}^k F_j} |0\rangle} \right).$$

(c) **Union (multi-source DCR).** For the disjunctive combination of $|m_1\rangle, \dots, |m_k\rangle$, the i -th output qubit is obtained via a negatively controlled NOT, followed by a correction X :

$$\begin{aligned} |\psi_0\rangle &= |m_1\rangle \dots |m_k\rangle |0\rangle, |\psi_1\rangle = C^{\{\overline{q_{i_1}}, \dots, \overline{q_{i_k}}\}} X(q_{i_{k+1}}) |\psi_0\rangle \rightarrow |m_1\rangle \dots |m_k\rangle \left(\sqrt{\sum_{F: \omega_{i+1} \in \cup_{j=1}^k F_j} |1\rangle} + \sqrt{\sum_{F: \omega_{i+1} \notin \cup_{j=1}^k F_j} |0\rangle} \right), \\ |\psi_2\rangle &= X(q_{i_{k+1}}) |\psi_1\rangle \longrightarrow \\ |m_1\rangle \dots |m_k\rangle &\left(\sqrt{\sum_{F: \omega_{i+1} \in \cup_{j=1}^k F_j} |1\rangle} + \sqrt{\sum_{F: \omega_{i+1} \notin \cup_{j=1}^k F_j} |0\rangle} \right). \end{aligned}$$

In the general BACR with multiple operation components and hierarchical layers, the output of each component is written to n ancilla qubits, which then serve as the input for the next layer.

Example 1: Consider two mass functions $m_1 = \{0.2, 0.1, 0.4, 0.3\}$ and $m_2 = \{0.05, 0.13, 0.02, 0.8\}$ and the Boolean operation $\mathfrak{B} = (F_{i_1} \cap F_{i_2}) \cup (\overline{F_{i_1}} \cap \overline{F_{i_2}})$. Based on the Definition 5, the output of BACR with \mathfrak{B} is $m_3 = \{0.229, 0.143, 0.357, 0.271\}$. Based on the Definition 6, the quantum circuit of implementing $|m_3\rangle$ from $|m_1\rangle$ and $|m_2\rangle$ is shown in Fig. 4. The measured probability vector of $q_{0_3}q_{1_3}$ is $[0.230, 0.143, 0.356, 0.271]^T$.

Theorem 2: For a Boolean algebra operation \mathfrak{B} , the squared amplitude of $|m_{k+1}\rangle$ constructed in Definition 6 coincides with the combined mass function m_{k+1} in Definition 5.

Proof 2: Please refer to the supplementary material.

Theorem 3: The CECR and DECR of two sources can be implemented on a quantum circuit without ancilla qubits,

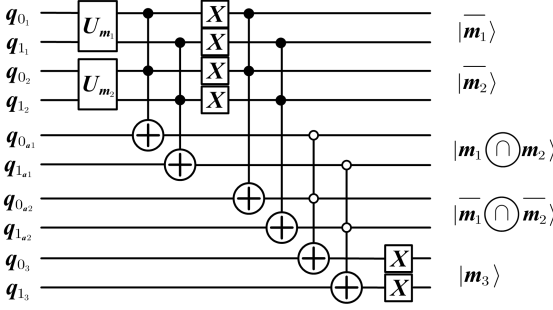


Fig. 4. Implementation of BACR on quantum circuits in Example 1, where q_{i_j} means the qubit which corresponds to ω_{i+1} in m_j , and a_j means the j th ancilla qubit.

which is more efficient than the general construction in Definition 6.

Proof 3: Please refer to the supplementary material.

Recalling our motivation, implementing BACR on quantum circuits is equivalent to quantize the Boolean algebra. The Boolean algebra is the theoretical basis of classical logical reasoning. Hence, from the above perspective, **the BACR can be viewed as the theoretical basis of quantum logical reasoning.**

B. α -junction on quantum circuits

Unlike general combination rules designed for specific tasks, the α -junction is a matrix calculus-based parametric combination rule derived from the specific requirements [35], [37]. Therefore, due to its extremely high computational complexity and the lack of interpretability for sources, it is often neglected in the context of information fusion under the belief function framework.

According to Eqs. (4)-(7), the α -junction can be written in a unified form as

$$m_1 \odot^\alpha m_2 = \sum_{F_i \subseteq \Omega} m_1(F_i) \mathbf{K}_{F_i}^{\cdot, \alpha} m_2 = \sum_{F_i \subseteq \Omega} m_1(F_i) \mathbf{m}_{2, F_i}^{\cdot, \alpha},$$

where $\cdot \in \{\cap, \cup\}$. Hence, the main sources of computational complexity are the construction of $\mathbf{K}_{F_i}^{\cdot, \alpha}$ and $\mathbf{m}_{2, F_i}^{\cdot, \alpha}$.

Theorem 4: The operator $\mathbf{K}_{F_i}^{\cdot, \alpha}$ can be realized as a Kronecker product of 2-dimensional matrices.

In the conjunctive case, the characteristic matrix is

$$\mathbf{C}^{\cap, \alpha} = \begin{bmatrix} \alpha & 1 \\ 1 - \alpha & 0 \end{bmatrix}, \mathbf{K}_{F_i}^{\cap, \alpha} = \bigotimes_{j=1}^{|\Omega|} \begin{cases} \mathbf{C}^{\cap, \alpha}, & \omega_{|\Omega|-j+1} \notin F_i, \\ \mathbf{I}_2, & \omega_{|\Omega|-j+1} \in F_i. \end{cases}$$

In the disjunctive case, the characteristic matrix is

$$\mathbf{C}^{\cup, \alpha} = \begin{bmatrix} 0 & 1 - \alpha \\ 1 & \alpha \end{bmatrix}, \mathbf{K}_{F_i}^{\cup, \alpha} = \bigotimes_{j=1}^{|\Omega|} \begin{cases} \mathbf{C}^{\cup, \alpha}, & \omega_{|\Omega|-j+1} \in F_i, \\ \mathbf{I}_2, & \omega_{|\Omega|-j+1} \notin F_i. \end{cases}$$

Proof 4: Please refer to the supplementary material.

According to Theorem 4, since $\mathbf{K}_{F_i}^{\cdot, \alpha}$ can be constructed via the Kronecker multiplication, this is the same way as the implementation of composite quantum systems. Therefore, it is a natural idea to implement the target matrix $\mathbf{K}_{F_i}^{\cdot, \alpha}$ on quantum circuits.

Definition 7: The conjunctive and disjunctive α -junction rules are

$$\sum_{F_i \subseteq \Omega} m_1(F_i) \mathbf{K}_{F_i}^{\cap, \alpha} m_2 = \sum_{F_i \subseteq \Omega} m_1(F_i) \mathbf{m}_{2, F_i}^{\cap, \alpha}, \quad (17)$$

$$\sum_{F_i \subseteq \Omega} m_1(F_i) \mathbf{K}_{F_i}^{\cup, \alpha} m_2 = \sum_{F_i \subseteq \Omega} m_1(F_i) \mathbf{m}_{2, F_i}^{\cup, \alpha}. \quad (18)$$

Suppose $|m_2\rangle$ is encoded on q_0, \dots, q_{n-1} , with ancillas $q_{0_a}, \dots, q_{(n-1)_a}$.

Conjunctive case. The evolution is

$$|\psi_0\rangle = |m_2\rangle |0\rangle^n, |\psi_1\rangle = X^{\otimes n} |\psi_0\rangle,$$

$$|\psi_2\rangle = \left(\prod_{i=0}^{n-1} C^{\{q_i\}} R_Y(2 \arccos \sqrt{\alpha})(q_{i_a}) \right) |\psi_1\rangle,$$

$$|\psi_3\rangle = X^{\otimes n} |\psi_2\rangle \longrightarrow |m_2^{\cap, \alpha}\rangle.$$

Disjunctive case. The evolution is

$$|\psi_0\rangle = |m_2\rangle |0\rangle^n,$$

$$|\psi_1\rangle = \left(\prod_{i=0}^{n-1} C^{\{q_i\}} R_Y(2 \arccos \sqrt{\alpha})(q_{i_a}) \right) |\psi_0\rangle,$$

$$|\psi_2\rangle = X_{q_{0_a}, \dots, q_{(n-1)_a}}^{\otimes n} |\psi_1\rangle \longrightarrow |m_2^{\cup, \alpha}\rangle.$$

For a focal set F_i , introduce $q_{n_a}, \dots, q_{(2n-1)_a}$, then

$$\begin{cases} C^{\{q_{j-1_a}\}} X(q_{2j-1_a}), & \omega_j \notin F_i, \\ C^{\{q_{j-1}\}} X(q_{2j-1_a}), & \omega_j \in F_i, \end{cases}$$

so that measuring $q_{n_a}, \dots, q_{(2n-1)_a}$ yields $\mathbf{m}_{2, F_i}^{\cap, \alpha}$ or $\mathbf{m}_{2, F_i}^{\cup, \alpha}$.

Example 2: Consider a mass function

$$m = \{0.02, 0.1, 0.1, 0.25, 0.06, 0.27, 0.02, 0.18\},$$

the state $|m_2^{\cap, \alpha}\rangle$ can be implemented based on the Definition 7, and the specific quantum circuit is shown in the Fig. 5. The

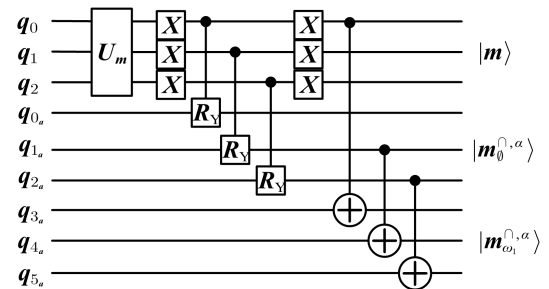


Fig. 5. Implementation of $|m_2^{\cap, 0.3}\rangle$ in Example 2, where $q_{0_a}, q_{1_a}, q_{2_a}$ compose the quantum state of $m_2^{\cap, 0.3}$ and $q_{3_a}, q_{4_a}, q_{5_a}$ compose the quantum state of $m_{\{\omega_1\}}^{\cap, \alpha}$.

measured probability vector with 8096 shots on $q_{0_a}, q_{1_a}, q_{2_a}$ and $q_{3_a}, q_{4_a}, q_{5_a}$ are

$$\begin{aligned} & [0.3657, 0.0461, 0.2205, 0.0345, 0.2297, 0.0493, 0.0473, 0.0069]^T, \\ & [0.0678, 0.3367, 0.0462, 0.21, 0.0726, 0.2054, 0.0121, 0.0492]^T, \end{aligned}$$

respectively. Based on the Eq. (17), when $\alpha = 0.3$, it has

$$m_{\emptyset}^{\cap,0.3} = \{0.3659, 0.0489, 0.2239, 0.0323, 0.2183, 0.0519, 0.0519, 0.0069\},$$

$$m_{\{\omega_1\}}^{\cap,0.3} = \{0.0698, 0.345, 0.0462, 0.21, 0.0742, 0.196, 0.0098, 0.049\}.$$

Theorem 5: For the same parameter α , the coefficient $m_{2,F_i}^{\cdot,\alpha}$ in the α -junction equals the squared amplitude of $|m_{2,F_i}^{\cdot,\alpha}\rangle$ in Definition 7.

Proof 5: Please refer to the supplementary material.

We implement $|m_{2,F_i}^{\cdot,\alpha}\rangle$ efficiently on a quantum circuit, which corresponds to the most computationally intensive step of the α -junction. Unlike classical operations, $|m_{2}^{\cdot,\alpha}\rangle$ encodes the information of all focal sets and allows repeated extraction via controlled operations on the corresponding qubits, avoiding redundant re-implementation. The subsequent vector-weighted summation in the α -junction can be completed on classical hardware.

Moreover, we propose an alternative implementation of the α -junction that requires fewer quantum gates and enables the entire procedure to be realized on quantum circuits. To clarify the construction, we briefly recall the definition of α -junction (Eqs. (4)–(8)). In the conjunctive case, the α -junction serves as an intermediate state between CECR and CCR, with α governing the interpolation. Since the implementations of CECR and CCR have been established in Definition 6 and Theorem 3, the intermediate state can be achieved by applying Control-RY gates to adjust between these two cases.

Definition 8: Consider two mass functions m_1 and m_2 , whose MFQSSs are $|m_1\rangle$ and $|m_2\rangle$ encoded on qubit registers q_{j_1}, q_{j_2} with $j = 0, \dots, n-1$. The α -junctions can be realized as follows.

Conjunctive case. Introduce $2n$ ancillas $q_{j_{a1}}, q_{j_{a2}}$. The state evolves as

$$|\psi_0\rangle = |m_1\rangle |m_2\rangle |0\rangle^{2n}, |\psi_1\rangle = X^{\otimes 2n} |\psi_0\rangle,$$

$$|\psi_2\rangle = \left(\prod_{j=0}^{n-1} C^{\{q_{j_1}, q_{j_2}\}} X(q_{j_{a1}}) \right) |\psi_1\rangle,$$

$$|\psi_3\rangle = \left(\prod_{j=0}^{n-1} C^{\{q_{j_1}\}} X(q_{j_{a2}}) C^{\{q_{j_2}\}} X(q_{j_{a2}}) \right) |\psi_2\rangle,$$

$$|\psi_4\rangle = X_{\{q_{j_{a2}}\}}^{\otimes n} |\psi_3\rangle \longrightarrow |m_1 \odot^{\alpha} m_2\rangle.$$

Disjunctive case. Introduce again $2n$ ancillas $q_{j_{a1}}, q_{j_{a2}}$. The evolution is

$$|\psi_0\rangle = |m_1\rangle |m_2\rangle |0\rangle^{2n}, |\psi_1\rangle = \left(\prod_{j=0}^{n-1} C^{\{q_{j_1}, q_{j_2}\}} X(q_{j_{a1}}) \right) |\psi_0\rangle,$$

$$|\psi_2\rangle = \left(\prod_{j=0}^{n-1} C^{\{q_{j_1}\}} X(q_{j_{a2}}) C^{\{q_{j_2}\}} X(q_{j_{a2}}) \right) |\psi_1\rangle \rightarrow |m_1 \odot^{\alpha} m_2\rangle.$$

The complete circuit for the above procedures is shown in Fig. 6.

This paper presents two implementations of the α -junction. The first is a partial realization on quantum circuits, motivated by its definition as a sequence of belief revisions applied to one input mass function, followed by weighted averaging with

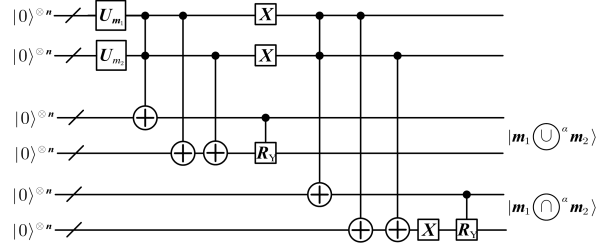


Fig. 6. Quantum implementation of the α -junctions.

another. The second is a full realization on quantum circuits, derived from the boundary conditions of the α -junction, where it can be regarded as an intermediate state between two non-parameterized rules. The first implementation provides a clearer physical interpretation of the α -junction and further inspires novel belief revision methods (see Section IV-D), while the second achieves lower gate complexity, as summarized in Table II.

C. Comparative analysis

In this paper, we achieve a quantized credal level without theoretical errors, owing to the mathematical consistency between the belief structure and the superposition state. Furthermore, we will demonstrate that BACR and α -junction require fewer computational resources on quantum circuits from the perspective of operation times.

Remark 5: In quantum computing, computational complexity can be evaluated in multiple ways, including circuit depth and the number of elementary gates. In this paper, we measure the complexity of evidence fusion by the number of Toffoli gates, while the complexity of belief revision for a single body of evidence is assessed by the number of single-control gates.

Theorem 6: Let m_1, \dots, m_k be k mass functions defined on an n -element FoD, with MFQSSs $|m_1\rangle, \dots, |m_k\rangle$. If the BACR corresponds to the Boolean operation $\mathfrak{B} = F_{i_1} \cap \dots \cap F_{i_k}$ (i.e., the multi-source CCR), then its quantum implementation requires $(k-1) \times n$ Toffoli gates.

Proof 6: Please refer to the supplementary material.

Theorem 7: In classical works, the computational complexity of combining k mass functions under an n -element FoD using CCR depends on the types of mass functions involved. For a poss-transferable mass function, the combination requires $(k-1) \times n$ multiplications, while for a general mass function, it requires $(k-1) \times 2^n$ multiplications.

Proof 7: Please refer to the supplementary material.

According to Theorems 6 and 7, we conclude that implementing CCR on quantum circuits yields no acceleration for poss-transferable mass functions, but provides exponential speedup for general mass functions. Remark 3 further explains this phenomenon from the perspective of quantum entanglement. In quantum circuits, logical operations are realized through control gates, which act not only on the information of individual qubits but also on their entanglement. By contrast, classical frameworks cannot intrinsically preserve or propagate entanglement through operations, requiring additional steps to simulate this effect. For poss-transferable mass functions, the

corresponding MFQS is a separable quantum state, meaning no entanglement exists among qubits; thus, quantum logical operations offer no advantage over classical methods. In contrast, general mass functions typically yield MFQSs that contain entanglement, enabling quantum circuits to achieve significant acceleration when performing logical operations.

Theorem 8: Consider a mass function m under an n -element FoD, with its MFQS represented as $|m\rangle$ in an n -qubit system. Implementing $|m^{\cdot,\alpha}\rangle$ requires n Control-RY gates, while extracting $|m_{F_0}^{\cdot,\alpha}\rangle \cdots |m_{F_{2^n-1}}^{\cdot,\alpha}\rangle$ requires $n \times 2^n$ C-NOT gates.

Proof 8: Please refer to the supplementary material.

Theorem 9: Consider two mass functions, m_1 and m_2 , under an n -element frame of discernment, with their MFQSs represented as $|m_1\rangle$ and $|m_2\rangle$. Implementing the α -junction rule in Definition 8 requires $4n$ operations.

Proof 9: Please refer to the supplementary material.

Theorem 10: In classical frameworks, the computational complexity of implementing $\mathbf{m}_{F_i}^{\cdot,\alpha}$ depends on the type of mass function. For the poss-transferable mass function, the implementations of $\mathbf{m}_{F_0}^{\cdot,\alpha}, \dots, \mathbf{m}_{F_{2^n-1}}^{\cdot,\alpha}$ require $n \times 2^n$ multiplications. For the general mass functions, the implementations of above require 2^{2n} multiplications.

Proof 10: Please refer to the supplementary material.

TABLE II

OPERATION TIMES IN CREDAL LEVEL OF CLASSICAL AND QUANTUM COMPUTATIONAL FRAMEWORKS.

	Classical	Quantum
Poss-transferable mass function (CCR)	$(k-1) \times n$	$(k-1) \times n$
General mass function (CCR)	$(k-1) \times 2^n$	$(k-1) \times n$
Poss-transferable mass function (partial α -junction)	$n \times 2^n$	$n \times 2^n$
General mass function (partial α -junction)	2^{2n}	$n \times 2^n$
Poss-transferable mass function (entire α -junction)	$n \times 2^n$	$4 \times n$
General mass function (entire α -junction)	2^{2n}	$4 \times n$

Table II presents a comparison of the computational complexity between classical and quantum frameworks from the perspective of CCR and α -junctions. When handling MFQSs with entangled information, i.e., MFQS of the general mass function, performing logic operations on quantum circuits can achieve exponential speedup without theoretical errors. Compared to other inference methods on quantum circuits [50], or belief transfer methods developed through general quantum algorithms [25], [32], **the proposed methods in this paper are more efficient, convenient, and logical, demonstrating that only belief functions can achieve these advantages on quantum circuits, as opposed to uncertainty theories under other structures.**

D. Modified credal level inspired by quantum computing

According to Definition 7, implementations on quantum circuits provide a more distinct interpretation for the meaning of the matrix $\mathbf{K}_{F_i}^{\cdot,\alpha}$ in α -junction. For the conjunctive case, when the matrix $\mathbf{K}_{\Omega \setminus \{\omega\}}^{\cdot,\alpha}$ acts on the vector \mathbf{m} , it is equivalent to first performing the negation operation on ω (apply X gate in quantum computing) and then adjusting the total belief masses of the element ω in the direction of the empty set, i.e., decreasing the belief masses of the focal sets with containing ω . Hence, when $\alpha = 0$, i.e., adjusting no belief masses, the

output $m_{\Omega \setminus \{\omega\}}^{\cap,0}(F_i) = \begin{cases} m(F_i \cup \{\omega\}) & \omega \notin F_i, \\ m(F_i \setminus \{\omega\}) & \omega \in F_i. \end{cases}$ And with

the α increasing, total belief masses of ω in $m_{\Omega \setminus \{\omega\}}^{\cap,\alpha}$ will be transferred to the empty set. Hence, it is not possible to realize $m_{\Omega \setminus \{\omega\}}^{\cap,\alpha} = m$ regardless of the value of alpha, which creates a significant obstacle to interpret this operation in practical applications. The similar phenomenon also appears in the disjunctive case. In this paper, we slightly modified this operation and propose a more reasonable and interpretable belief revision method.

Definition 9: Let an agent's knowledge state be represented by a mass function m over the FoD Ω . When external testimony suggests that the belief masses of elements in a subset F_i should be adjusted, the following revision operators are defined.

Contour enhancement revision (CER). If the testimony indicates that the masses in F_i should be *enhanced* with degree β , then

$$\mathbf{m}_{F_i}^{+,\beta} = \mathbf{K}_{F_i}^{+,\beta} \cdot \mathbf{m}, \quad (19)$$

with the revision matrix

$$\mathbf{K}_{F_i}^{+,\beta} = \bigotimes_{k=1}^{|\Omega|} \begin{cases} \mathbf{E}^\beta, & \omega_{\Omega-k+1} \in F_i, \\ \mathbf{I}_2, & \omega_{\Omega-k+1} \notin F_i, \end{cases} \quad \mathbf{E}^\beta = \begin{bmatrix} 1-\beta & 0 \\ \beta & 1 \end{bmatrix}. \quad (20)$$

Contour reduction revision (CRR). If the testimony indicates that the masses in F_i should be *reduced* with degree β , then

$$\mathbf{m}_{F_i}^{-,\beta} = \mathbf{K}_{F_i}^{-,\beta} \cdot \mathbf{m}, \quad (21)$$

with the revision matrix

$$\mathbf{K}_{F_i}^{-,\beta} = \bigotimes_{k=1}^{|\Omega|} \begin{cases} \mathbf{R}^\beta, & \omega_{\Omega-k+1} \in F_i, \\ \mathbf{I}_2, & \omega_{\Omega-k+1} \notin F_i, \end{cases} \quad \mathbf{R}^\beta = \begin{bmatrix} 1 & \beta \\ 0 & 1-\beta \end{bmatrix}. \quad (22)$$

Similar with the α -junction, the CER and CRR also can be implemented on quantum circuits efficiently.

Definition 10: Let the MFQS $|m\rangle$ of a mass function m be prepared on qubits q_0, \dots, q_{n-1} . Introduce ancillas $q_{0_a}, \dots, q_{(n-1)_a}$ for the following operations.

CER: The state evolves as

$$|\psi_0\rangle = |m\rangle |0\rangle^n, |m^{-,\beta}\rangle = \left(\prod_{i=0}^{n-1} C^{\{q_i\}} R_Y(2 \arccos(\sqrt{\beta}))(q_{i_a}) \right) |\psi_0\rangle,$$

For a focal set F_i , introduce additional ancillas $q_{n_a}, \dots, q_{(2n-1)_a}$ and apply

$$\begin{cases} C^{\{q_{j-1_a}\}} X(q_{2j-1_a}), & \omega_j \in F_i, \\ C^{\{q_{j-1}\}} X(q_{2j-1_a}), & \omega_j \notin F_i, \end{cases} \quad j = 1, \dots, n,$$

so that measuring $q_{n_a}, \dots, q_{(2n-1)_a}$ yields $\mathbf{m}_{F_i}^{-,\beta}$.

CRR: Similarly, the evolution is

$$|\psi_0\rangle = |m\rangle |0\rangle^n, |\psi_1\rangle = \left(\prod_{i=0}^{n-1} C^{\{\bar{q_i}\}} R_Y(2 \arccos(\sqrt{\beta}))(q_{i_a}) \right) |\psi_0\rangle,$$

$$|\psi_2\rangle = X_{\{q_{0_a}, \dots, q_{(n-1)_a}\}}^{\otimes n} |\psi_1\rangle, |\psi_3\rangle = |m^{+,\beta}\rangle.$$

For a focal set F_i , introduce $q_{n_a}, \dots, q_{(2n-1)_a}$ and apply

$$\begin{cases} C^{\{q_{j-1_a}\}} X(q_{2j-1_a}), & \omega_j \in F_i, \\ C^{\{q_{j-1}\}} X(q_{2j-1_a}), & \omega_j \notin F_i, \end{cases} \quad j = 1, \dots, n,$$

so that measuring $q_{n_a}, \dots, q_{(2n-1)_a}$ yields $\mathbf{m}_{F_i}^{+, \beta}$.

Compared to the matrix calculus in α -junction, the proposed revision method offers a clearer physical interpretation. CER and CRR enable the enhancement or reduction of the belief masses of selected elements without impacting others. In this paper, our goal is to demonstrate that quantum computing can inspire novel approaches to belief revision. The specific properties and performance of CER and CRR will be explored in future works.

V. OPERATIONS ON PRODUCT SPACE ON QUANTUM CIRCUITS

In the preceding discussion, the advantages of belief functions on quantum circuits have been demonstrated from the perspective of operations within a FoD. For the operations on product space, they also can be efficiently implemented on quantum circuits.

A. Marginalization on quantum circuits

Definition 11: Consider a mass function on the product frame $\Omega \times \Theta$, denoted $m^{\Omega \times \Theta}$, whose MFQS $|m^{\Omega \times \Theta}\rangle$ is implemented in a $|\Omega| \times |\Theta|$ -qubit register $q_{(0,0)}, q_{(0,1)}, \dots, q_{(|\Omega|-1,|\Theta|-1)}$, where $q_{(i,j)}$ encodes the element $(\omega_{i+1}, \theta_{j+1})$. The marginalization of $m^{\Omega \times \Theta}$ on Ω can be realized as follows.

$$|\psi_0\rangle = |m^{\Omega \times \Theta}\rangle |0\rangle^{|\Omega|}, |\psi_1\rangle = \left(\prod_{i=0}^{|\Omega|-1} C^{\{q_{(i,0)}, \dots, q_{(i,|\Theta|-1)}\}} X(q_{i_a}) \right) |\psi_0\rangle,$$

$$|\psi_2\rangle = X^{\otimes |\Omega|}_{\{q_{0_a}, \dots, q_{(|\Omega|-1)_a}\}} |\psi_1\rangle, |\psi_3\rangle \rightarrow |m^{\Omega \times \Theta \downarrow \Omega}\rangle,$$

where $q_{0_a}, \dots, q_{(|\Omega|-1)_a}$ are the ancilla qubits carrying the marginalized distribution.

Example 3: Consider a mass function

$$m^{\Omega \times \Theta} \equiv \{m^{\Omega \times \Theta}((\omega_1, \theta_1)) = 0.1, m^{\Omega \times \Theta}((\omega_1, \theta_2), (\omega_2, \theta_2)) = 0.4, m^{\Omega \times \Theta}((\omega_1, \theta_1), (\omega_2, \theta_1), (\omega_2, \theta_2)) = 0.2, m^{\Omega \times \Theta}(\Omega \times \Theta) = 0.3\},$$

according to the Eq. (11), the marginalization of $m^{\Omega \times \Theta}$ on Ω and Θ are

$$m^{\Omega \times \Theta \downarrow \Omega}(\{\omega_1\}) = 0.3, m^{\Omega \times \Theta \downarrow \Omega}(\Omega) = 0.7; \\ m^{\Omega \times \Theta \downarrow \Theta}(\{\theta_1\}) = 0.1, m^{\Omega \times \Theta \downarrow \Theta}(\{\theta_2\}) = 0.4, m^{\Omega \times \Theta \downarrow \Theta}(\Theta) = 0.5.$$

Based on the Definition 11, its quantum circuits are shown in Fig. 7, and the probability measures of $q_{0_a} q_{1_a}$ and $q_{2_a} q_{3_a}$ are

$$Prob_{q_{0_a} q_{1_a}}(|01\rangle) = 0.3, Prob_{q_{0_a} q_{1_a}}(|11\rangle) = 0.7; \\ Prob_{q_{2_a} q_{3_a}}(|01\rangle) = 0.1, Prob_{q_{2_a} q_{3_a}}(|10\rangle) = 0.4, \\ Prob_{q_{2_a} q_{3_a}}(|11\rangle) = 0.5.$$

Theorem 11: The squared amplitudes of the output state $|m^{\Omega \times \Theta \downarrow \Omega}\rangle$ in Definition 11 equal the outcome of marginalization in Eq. (10).

Proof 11: Please refer to the supplementary material.

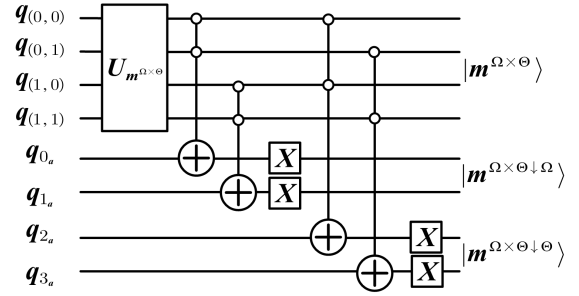


Fig. 7. Implementation of $|m^{\Omega \times \Theta \downarrow \Omega}\rangle$ and $|m^{\Omega \times \Theta \downarrow \Theta}\rangle$ in Example 3.

B. Vacuous extension on quantum circuits

Definition 12: Consider a mass function m^Ω under the FoD Ω , with MFQS $|m^\Omega\rangle$ implemented in an $|\Omega|$ -qubit system $q_0, \dots, q_{|\Omega|-1}$, where q_i corresponds to element ω_{i+1} . The vacuous extension of m^Ω to $\Omega \times \Theta$ can be realized as follows.

$$|\psi_0\rangle = |m^\Omega\rangle |0\rangle^{|\Omega| \cdot |\Theta|}, \\ |m^{\Omega \uparrow \Omega \times \Theta}\rangle = \left(\prod_{i=0}^{|\Omega|-1} \prod_{j=0}^{|\Theta|-1} C^{\{q_i\}} X(q_{(i,j)_a}) \right) |\psi_0\rangle,$$

where $q_{(i,j)_a}$ denotes the state of the composite element $(\omega_{i+1}, \theta_{j+1}) \in \Omega \times \Theta$.

Example 4: Consider a mass function under the FoD Ω ,

$$m^\Omega(\{\omega_1\}) = 0.1, m^\Omega(\{\omega_2\}) = 0.4, m^\Omega(\Omega) = 0.5.$$

According to Eq. (12), its vacuous extension on FoD $\Omega \times \Theta$ is

$$m^{\Omega \uparrow \Omega \times \Theta}((\omega_1, \theta_1), \dots, (\omega_1, \theta_{|\Theta|})) = 0.1, m^{\Omega \uparrow \Omega \times \Theta}((\omega_2, \theta_1), \dots, (\omega_2, \theta_{|\Theta|})) = 0.4, m^{\Omega \uparrow \Omega \times \Theta}(\Omega \times \Theta) = 0.5.$$

Based on the Definition 12, the circuit of implementing MFQS of $m^{\Omega \uparrow \Omega \times \Theta}$ is shown in Figure 8, and the probability measures of $q_{(0,0)_a} \dots q_{(1,|\Theta|-1)_a}$ are

$$Prob_{q_{(0,0)_a} \dots q_{(1,|\Theta|-1)_a}}(|0_{|\Theta|} 1_{|\Theta|}\rangle) = 0.1, \\ Prob_{q_{(0,0)_a} \dots q_{(1,|\Theta|-1)_a}}(|1_{|\Theta|} 0_{|\Theta|}\rangle) = 0.4, \\ Prob_{q_{(0,0)_a} \dots q_{(1,|\Theta|-1)_a}}(|1_{2 \times |\Theta|}\rangle) = 0.5.$$

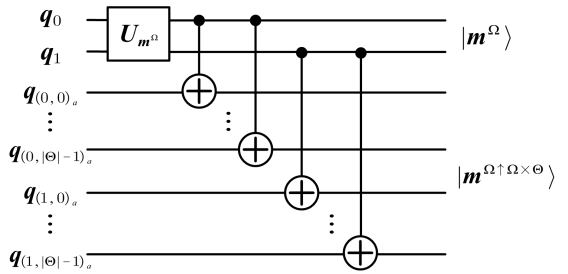


Fig. 8. Implementation of $|m^{\Omega \uparrow \Omega \times \Theta}\rangle$ in Example 4.

Theorem 12: The squared amplitudes of the output state $|m^{\Omega \uparrow \Omega \times \Theta}\rangle$ in Definition 12 equal the outcome of vacuous extension in Eq. (12).

Proof 12: Please refer to the supplementary material.

C. Ballooning extension on quantum circuits

Definition 13: Consider a mass function with a fixed subset $F_i \subseteq \Theta$ under an FoD Ω , denoted $m^\Omega[F_i]$. Its MFQS $|m^\Omega[F_i]\rangle$ is implemented in an $|\Omega|$ -qubit register $q_0, \dots, q_{|\Omega|-1}$, where q_k corresponds to element ω_{k+1} . The ballooning extension of $m^\Omega[F_i]$ to $\Omega \times \Theta$ can be realized as follows.

$$|\psi_0\rangle = |m^\Omega[F_i]\rangle |0\rangle^{|\Omega|-|\Theta|},$$

$$|\psi_1\rangle = \left(\prod_{\theta_j \in F_i} \prod_{k=0}^{|\Omega|-1} C^{\{q_k\}} X(q_{(k,j)_a}) \right) |\psi_0\rangle,$$

$$|m^\Omega[F_i] \uparrow \Omega \times \Theta\rangle = \left(\prod_{\theta_j \notin F_i} X^{\otimes |\Omega|}_{\{q_{(0,j)_a}, \dots, q_{(|\Omega|-1,j)_a}\}} \right) |\psi_1\rangle,$$

where $q_{(k,j)_a}$ encodes the composite element $(\omega_{k+1}, \theta_{j+1}) \in \Omega \times \Theta$.

Example 5: Consider a mass function with given θ_2 under the FoD Ω ,

$$m^\Omega[\{\theta_2\}](\{\omega_1\}) = 0.1, m^\Omega[\{\theta_2\}](\{\omega_2\}) = 0.4, m^\Omega[\{\theta_2\}](\Omega) = 0.5.$$

According to Eq.(13), its ballooning extension on the FoD $\Omega \times \Theta$ is

$$m^\Omega[\{\theta_2\}] \uparrow \Omega \times \Theta((\omega_1, \theta_2), (\omega_2, \theta_1), (\omega_2, \theta_2)) = 0.1,$$

$$m^\Omega[\{\theta_2\}] \uparrow \Omega \times \Theta((\omega_1, \theta_1), (\omega_1, \theta_2), (\omega_2, \theta_2)) = 0.4,$$

$$m^\Omega[\{\theta_2\}] \uparrow \Omega \times \Theta(\Omega \times \Theta) = 0.5.$$

Based on the Definition 13, the circuit of implementing MFQS of $m^\Omega[\{\theta_2\}] \uparrow \Omega \times \Theta$ is shown in Figure 9, and the probability measures of $q_{(0,0)_a} \dots q_{(1,1)_a}$ are

$$\begin{aligned} \text{Prob}_{q_{(0,0)_a} \dots q_{(1,1)_a}}(|1110\rangle) &= 0.1, \\ \text{Prob}_{q_{(0,0)_a} \dots q_{(1,1)_a}}(|1011\rangle) &= 0.4, \\ \text{Prob}_{q_{(0,0)_a} \dots q_{(1,1)_a}}(|1111\rangle) &= 0.5. \end{aligned}$$

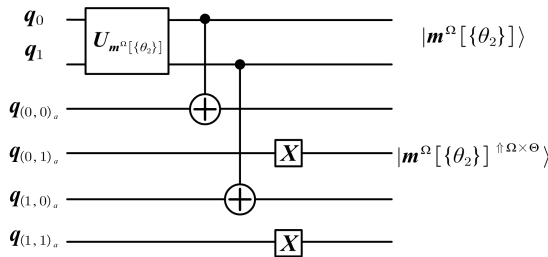


Fig. 9. Implementation of $|m^\Omega[\{\theta_2\}] \uparrow \Omega \times \Theta\rangle$ in Example 5.

Theorem 13: The square of amplitude output state $|m^\Omega[\{\theta_2\}] \uparrow \Omega \times \Theta\rangle$ in Definition 13 equals the outcome of ballooning extension in Eq. (13).

Proof 13: Please refer to the supplementary material.

D. Generalized Bayesian theorem on quantum circuits

Unlike the credal and pignistic levels in the TBM, operations on the product space involve re-encoding the information granule. In the classical framework, this re-encoding is performed through projection, multiplication, and set operations, which complicates arithmetic and programming in large-scale computing. In this paper, these re-encoding operations are efficiently implemented on quantum circuits and are generalizable to accommodate more complex computations. The VBS [43] and the GBT [42] are the most well-known tools for reasoning and decision making with multiple variables under the belief function frameworks. In the VBS, combining the bodies of evidence under the different FoDs and the marginalization are the key steps. In the GBT, the conditional embedding in the product space (ballooning extension) and the Dempster's conditioning are the key steps. Since the aforementioned techniques have been implemented in this paper, both VBS and GBT can also be extended to quantum circuits, making the operations more convenient.

To verify the effectiveness of the proposed method, we implement the example from [51] on quantum circuits, which uses GBT to compute a Bayesian network. Consider four variables **IR**, **OI**, **SM** and **SP**, and their true value are located in the frame \mathcal{IR} , \mathcal{OI} , \mathcal{SM} and \mathcal{SP} , respectively. When they are binary variables and the restrictions are Bayesian mass functions, the network and their restrictions are shown in Fig. 10.

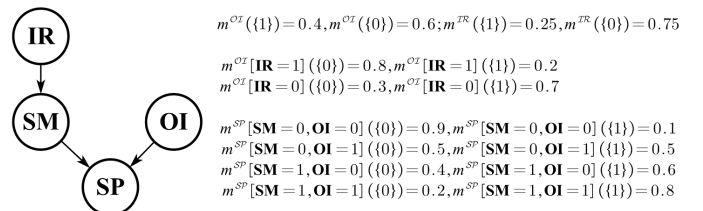


Fig. 10. Four nodes Bayesian network and their restrictions.

Borujeni *et al.* [51] implemented the aforementioned network on a quantum circuit using the probabilistic framework via Low's method [50]. Building on the proposed TBM (Transferable Belief Model) for quantum circuits, the network can also be realized under the belief structure, with the specific circuit presented in Section 2 of the supplementary material. Since Low's method uses a qubit to represent a binary variable, it cannot be extended to general mass functions, such as multi-dimensional probability distributions or mass functions with multi-element focal sets. However, under the belief structure—where each element is encoded as a qubit—the circuit shown in the supplementary material can accommodate these extended cases.

VI. CONCLUSION

This pioneering paper establishes a correspondence encoding between qubits in quantum computing and elements of the Dempster-Shafer structure, demonstrating that quantum circuit operations can significantly enhance the efficiency of belief function computations. Compared to the direct extension of

classical probability to quantum probability, belief function operations are more logically suited to quantum computing and provide a clearer interpretation of qubits in reasoning and decision-making. Furthermore, inspired by the application of belief functions on quantum circuits, we introduce a novel belief revision method, called contour enhancement/reduction revision, which offers a previously unexplored reasoning semantics.

This paper also validates the issue raised in the introduction: **developing quantum AI methods within the belief function framework offers greater interpretability and generalizability compared to other uncertainty theories.** Moving forward, future research will proceed in two directions. First, we will explore broader advantages of belief functions on quantum circuits, including applications such as evidential machine learning and evidential deep learning. Second, we propose utilizing belief functions as the foundational representation for quantum AI information, aiming to optimize existing quantum AI models.

REFERENCES

- [1] R. R. Yager and L. Liu, *Classic works of the Dempster-Shafer theory of belief functions*. Springer, 2008, vol. 219.
- [2] P. Smets and R. Kennes, “The transferable belief model,” *Artificial Intelligence*, vol. 66, no. 2, pp. 191–234, 1994.
- [3] J.-B. Yang and D.-L. Xu, “Evidential reasoning rule for evidence combination,” *Artificial Intelligence*, vol. 205, pp. 1–29, 2013.
- [4] Y. Zhang, S. Destercke, Z. Zhang, T. Bouadi, and A. Martin, “On computing evidential centroid through conjunctive combination: An impossibility theorem,” *IEEE Transactions on Artificial Intelligence*, vol. 4, no. 3, pp. 487–496, 2023.
- [5] M. Zhou, Y.-J. Zhou, J.-B. Yang, and J. Wu, “A generalized belief dissimilarity measure based on weighted conflict belief and distance metric and its application in multi-source data fusion,” *Fuzzy Sets and Systems*, vol. 475, p. 108719, 2024.
- [6] J. Zhao and K. H. Cheong, “Mase: Multi-attribute source estimator for epidemic transmission in complex networks,” *IEEE Transactions on Systems, Man, and Cybernetics: Systems*, 2024.
- [7] J. Deng, Y. Deng, and J.-B. Yang, “Random permutation set reasoning,” *IEEE Transactions on Pattern Analysis and Machine Intelligence*, 2024.
- [8] X. Chen and Y. Deng, “Evidential software risk assessment model on ordered frame of discernment,” *Expert Systems with Applications*, vol. 250, p. 123786, 2024.
- [9] Z. Liu, C. Li, and X. He, “Evidential ensemble preference-guided learning approach for real-time multimode fault diagnosis,” *IEEE Transactions on Industrial Informatics*, vol. 20, no. 4, pp. 5495–5504, 2024.
- [10] Z. Zhang, Z. Liu, H. Tian, and A. Martin, “Mixed-type imputation for missing data credal classification via quality matrices,” *IEEE Transactions on Systems, Man, and Cybernetics: Systems*, vol. 54, no. 8, pp. 4772–4785, 2024.
- [11] L. Huang, J. Fan, and A. W.-C. Liew, “Integration of multikinds imputation with covariance adaptation based on evidence theory,” *IEEE Transactions on Neural Networks and Learning Systems*, pp. 1–15, 2024.
- [12] L. Huang, S. Ruan, P. Decazes, and T. Denœux, “Deep evidential fusion with uncertainty quantification and reliability learning for multimodal medical image segmentation,” *Information Fusion*, vol. 113, p. 102648, 2025.
- [13] S. Barhoumi, I. K. Kallel, É. Bossé, and B. Solaiman, “An empirical survey-type analysis of uncertainty measures for the fusion of crisp and fuzzy bodies of evidence,” *Information Fusion*, vol. 121, p. 103106, 2025.
- [14] D. Dong, C. Chen, H. Li, and T.-J. Tarn, “Quantum reinforcement learning,” *IEEE Transactions on Systems, Man, and Cybernetics, Part B (Cybernetics)*, vol. 38, no. 5, pp. 1207–1220, 2008.
- [15] J. Biamonte, P. Wittek, N. Pancotti, P. Rebentrost, N. Wiebe, and S. Lloyd, “Quantum machine learning,” *Nature*, vol. 549, p. 195–202, 2017.
- [16] D. Dong, X. Xing, H. Ma, C. Chen, Z. Liu, and H. Rabitz, “Learning-based quantum robust control: algorithm, applications, and experiments,” *IEEE transactions on cybernetics*, vol. 50, no. 8, pp. 3581–3593, 2019.
- [17] J. Li, J. Zhang, J. Zhang, and S. Zhang, “Quantum knn classification with k value selection and neighbor selection,” *IEEE Transactions on Computer-Aided Design of Integrated Circuits and Systems*, vol. 43, no. 5, pp. 1332–1345, 2024.
- [18] A. Abbas, D. Sutter, C. Zoufal, A. Lucchi, A. Figalli, and S. Woerner, “The power of quantum neural networks,” *Nature Computational Science*, vol. 1, no. 6, pp. 403–409, 2021.
- [19] G. Gentilletta, A. Thomsen, D. Sutter, and S. Woerner, “The complexity of quantum support vector machines,” *Quantum*, vol. 8, p. 1225, 2024.
- [20] Y. Wang, B. Qi, X. Wang, T. Liu, and D. Dong, “Power characterization of noisy quantum kernels,” *IEEE Transactions on Neural Networks and Learning Systems*, 2025.
- [21] D. Dong and I. R. Petersen, “Machine learning for quantum control,” in *Learning and Robust Control in Quantum Technology*. Springer, 2023, pp. 93–140.
- [22] S. Chen, J. Cotler, H.-Y. Huang, and J. Li, “The complexity of nisq,” *Nature Communications*, vol. 14, no. 1, p. 6001, 2023.
- [23] T. Li, L. Lu, Z. Zhao, Z. Tan, S. Tan, and J. Yin, “Qust: Optimizing quantum neural network against spatial and temporal noise biases,” *IEEE Transactions on Computer-Aided Design of Integrated Circuits and Systems*, vol. 44, no. 4, pp. 1434–1447, 2025.
- [24] J. Von Neumann, *Mathematical foundations of quantum mechanics: New edition*. Princeton university press, 2018, vol. 53.
- [25] Q. Zhou, G. Tian, and Y. Deng, “Bf-qc: Belief functions on quantum circuits,” *Expert Systems with Applications*, vol. 223, p. 119885, 2023.
- [26] A. Vourdas, “Quantum probabilities as Dempster-Shafer probabilities in the lattice of subspaces,” *Journal of Mathematical Physics*, vol. 55, no. 8, p. 082107, 08 2014.
- [27] F. Xiao, “Generalized quantum evidence theory,” *Applied Intelligence*, vol. 53, no. 11, pp. 14 329–14 344, 2023.
- [28] L. Pan, X. Gao, and Y. Deng, “Quantum algorithm of dempster rule of combination,” *Applied Intelligence*, vol. 53, no. 8, pp. 8799–8808, 2023.
- [29] X. Deng, S. Xue, and W. Jiang, “A novel quantum model of mass function for uncertain information fusion,” *Information Fusion*, vol. 89, pp. 619–631, 2023.
- [30] X. Deng and W. Jiang, “Quantum representation of basic probability assignments based on mixed quantum states,” in *2021 IEEE 24th International Conference on Information Fusion (FUSION)*. IEEE, 2021, pp. 1–6.
- [31] L. Pan and X. Gao, “Evidential markov decision-making model based on belief entropy to predict interference effects,” *Information Sciences*, vol. 633, pp. 10–26, 2023.
- [32] H. Luo, Q. Zhou, Z. Li, and Y. Deng, “Variational quantum linear solver-based combination rules in dempster–shafer theory,” *Information Fusion*, vol. 102, p. 102070, 2024.
- [33] H. Luo, Q. Zhou, L. Pan, Z. Li, and Y. Deng, “Attribute fusion-based evidential classifier on quantum circuits,” *arXiv preprint arXiv:2401.01392*, 2024.
- [34] G. Shafer, *A Mathematical Theory of Evidence*. Princeton University Press, 1976.
- [35] P. Smets, “The application of the matrix calculus to belief functions,” *International Journal of Approximate Reasoning*, vol. 31, no. 1, pp. 1–30, 2002.
- [36] T. Denœux, “Conjunctive and disjunctive combination of belief functions induced by nondistinct bodies of evidence,” *Artificial Intelligence*, vol. 172, no. 2–3, pp. 234–264, 2008.
- [37] F. Pichon and T. Denœux, “Interpretation and Computation of alpha-Junctions for Combining Belief Functions,” in *6th International Symposium on Imprecise Probability: Theories and Applications (ISIPTA '09)*, Durham, United Kingdom, 2009. [Online]. Available: <https://hal.science/hal-00450984>
- [38] P. Smets, “Decision making in the tbm: the necessity of the pignistic transformation,” *International Journal of Approximate Reasoning*, vol. 38, no. 2, pp. 133–147, 2005.
- [39] D. Han, J. Dezert, and Z. Duan, “Evaluation of probability transformations of belief functions for decision making,” *IEEE Transactions on Systems, Man, and Cybernetics: Systems*, vol. 46, no. 1, pp. 93–108, 2016.
- [40] B. R. Cobb and P. P. Shenoy, “On the plausibility transformation method for translating belief function models to probability models,” *International Journal of Approximate Reasoning*, vol. 41, no. 3, pp. 314–330, 2006.
- [41] T. Denœux and P. Smets, “Classification using belief functions: Relationship between case-based and model-based approaches,” *IEEE Transactions on Systems, Man, and Cybernetics, Part B (Cybernetics)*, vol. 36, no. 6, pp. 1395–1406, 2006.

- [42] P. Smets, “Belief functions: The disjunctive rule of combination and the generalized bayesian theorem,” *International Journal of Approximate Reasoning*, vol. 9, no. 1, pp. 1–35, 1993.
- [43] P. P. Shenoy and G. Shafer, “Axioms for probability and belief-function propagation,” in *Uncertainty in Artificial Intelligence*, ser. Machine Intelligence and Pattern Recognition, R. D. SHACHTER, T. S. LEVITT, L. N. KANAL, and J. F. LEMMER, Eds. North-Holland, 1990, vol. 9, pp. 169–198.
- [44] M. A. Nielsen and I. Chuang, “Quantum computation and quantum information,” 2002.
- [45] L. Pan and Y. Deng, “A new complex evidence theory,” *Information Sciences*, vol. 608, pp. 251–261, 2022. [Online]. Available: <https://www.sciencedirect.com/science/article/pii/S0020025522006570>
- [46] F. Xiao, Z. Cao, and C.-T. Lin, “A complex weighted discounting multi-source information fusion with its application in pattern classification,” *IEEE Transactions on Knowledge and Data Engineering*, vol. 35, no. 8, pp. 7609–7623, 2023.
- [47] Q. Zhou, Y. Deng, and R. R. Yager, “Cd-bft: Canonical decomposition-based belief functions transformation in possibility theory,” *IEEE Transactions on Cybernetics*, vol. 54, no. 1, pp. 611–623, 2024.
- [48] Q. Zhou, H. Luo, É. Bossé, and Y. Deng, “Why combining belief functions on quantum circuits?” in *Belief Functions: Theory and Applications*, Y. Bi, A.-L. Jousselme, and T. Denoeux, Eds. Cham: Springer Nature Switzerland, 2024, pp. 161–170.
- [49] F. Pichon, S. Destercke, and T. Burger, “A consistency-specificity trade-off to select source behavior in information fusion,” *IEEE Transactions on Cybernetics*, vol. 45, no. 4, pp. 598–609, 2015.
- [50] G. H. Low, T. J. Yoder, and I. L. Chuang, “Quantum inference on bayesian networks,” *Physical Review A*, vol. 89, no. 6, p. 062315, 2014.
- [51] S. E. Borujeni, S. Nannapaneni, N. H. Nguyen, E. C. Behrman, and J. E. Steck, “Quantum circuit representation of bayesian networks,” *Expert Systems with Applications*, vol. 176, p. 114768, 2021.